

Age-Invariant Face Embedding using the Wasserstein Distance

Eran Dahan and Yosi Keller



Abstract—In this work, we study face verification in datasets where images of the same individuals exhibit significant age differences. This poses a major challenge for current face recognition and verification techniques. To address this issue, we propose a novel approach that utilizes multitask learning and a Wasserstein distance discriminator to disentangle age and identity embeddings of facial images. Our approach employs multitask learning with a Wasserstein distance discriminator that minimizes the mutual information between the age and identity embeddings by minimizing the Jensen-Shannon divergence. This improves the encoding of age and identity information in face images and enhances the performance of face verification in age-variant datasets. We evaluate the effectiveness of our approach using multiple age-variant face datasets and demonstrate its superiority over state-of-the-art methods in terms of face verification accuracy.

1 INTRODUCTION

Face recognition and verification are fundamental tasks in computer vision, with a wide range of applications in security, surveillance, and human-computer interaction. A number of techniques have been suggested enhancing the accuracy of facial recognition, including the computation of face features through learning [41], [40], as well as the use of deep learning methods [32], [42] and training losses such as the Triplet [35] and Large Margin losses [13], [45], [4]. Although these methods have been effective, changes in appearance caused by age, pose, and lighting conditions can significantly decrease their accuracy. Therefore, facial recognition systems strive to increase the separation between different identities (interclass separation) while decreasing the separation between images of the same identity (intraclass separation). Age-invariant face verification is a crucial component of some facial recognition tasks, with many applications, including locating missing children [5], [11], medical uses [2], [30], kinship verification [28], [46], and demographic estimation [37], among others. However, the age-related variations in facial appearance (see Fig. 1 of the Appendix) might be significant as the age gap between the images increases. For instance, using face images taken decades earlier for face verification, decreases the verification accuracy in real-world datasets. Various methods have been proposed to address age-invariant face verification, which can be broadly categorized as intraclass

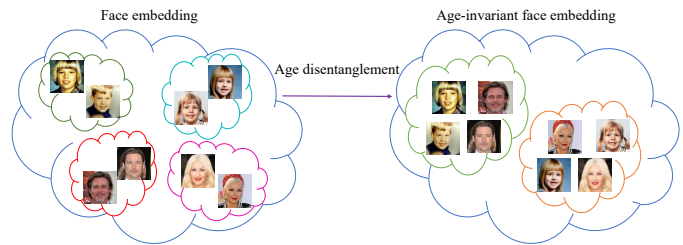


Fig. 1: Age and identity disentanglement. The left-hand side shows the common face embedding space that encodes both age and identity, with the embeddings of each person grouped separately by age. The right-hand side shows an age-invariant embedding, in which all images of the same person are grouped together, regardless of their substantial age differences.

minimization, face synthesis, and disentanglement methods. Face synthesis methods synthesize face images of the same subjects (identities) at different ages to enlarge the training set per identity and reflect the aging effect [11], [52], [22]. These methods are based on using generative adversarial networks (GANs). However, although GANs have made significant improvements in recent years, such methods only enlarge the training dataset and do not improve the image embeddings. Recent methods for age-invariant face verification apply statistical disentanglement to disentangle the biometric attributes, as shown in Fig. 1. In most cases, as in age disentanglement, the attribute we wish to disentangle from the image embedding is not linearly separable from the other biometric face attributes. Given a face image x , its embedding \hat{x} , with identity and age attributes x_{id} , x_{age} , respectively, there is no straightforward analytical formulation to separate x_{id} or x_{age} from \hat{x} . Additionally, it is difficult to model the relationship between these two attributes, requiring statistical disentanglement methods. Thus, various disentanglement methods have been proposed, including probabilistic models [17], Expectation Maximization (EM) techniques [18], and gradient orientation pyramids [27].

In this work, we propose to improve the statistical disentanglement of the age and identity attributes of face images. We derive an age-invariant identity embedding x_{id} that is invariant to the age attribute x_{age} . For that, we propose a novel method to disentangle the age and identity features with respect to their mutual information.

• E. Dahan & Y. Keller are with the Faculty of Engineering, Bar-Ilan University, Email:yosi.keller@gmail.com

Manuscript received April 19, 2005; revised August 26, 2015.

Statistical disentanglement was first studied by Independent Component Analysis (ICA) [16], [23] optimizing statistical divergence measures between the estimated signals. Recent work by Huo et al. [19] and Xie et al. [50] also considered minimizing mutual information to disentangle age and identity through neural estimation. In contrast, our approach utilizes a multitask learning architecture with a Wasserstein distance discriminator that minimizes the Jensen-Shannon divergence. We denote the resulting age-invariant face image embedding as the Wasserstein Mutual Information for Age Invariant (WMI-AI). Our method is shown to effectively reduce the mutual information between age and identity embeddings, and is similar to the use of the Wasserstein distance as a discriminator to stabilize WGAN training [1], or as a discriminator for domain adaptation [38].

In particular, we propose the following contributions:

- We propose a multitask learning architecture that disentangles the age and identity embeddings while optimizing the embeddings for age classification and face recognition.
- We suggest a discriminator based on the Wasserstein distance and Jensen-Shannon divergence to minimize the mutual information between the embedding tasks.
- Through extensive evaluation of major cross-age face verification datasets, including CALFW [53], AgeDB30 [31], CACD-VS [6], and ECAF [22], we demonstrate that our method achieves state-of-the-art accuracy, even when the age gap between the pair of compared images is significant.

2 RELATED WORK

2.1 Age-Invariant Face Image Embedding

Learning the aging patterns in face images. Some researchers have focused on learning the manifestation of the aging process in face images. Park et al. [33] proposed a 3D face age model to compensate for age variations in 2D probe face images. Ramanathan et al. [34] suggested a shape transformation model to model the aging process. However, these methods require large annotated datasets to achieve high performance.

Face synthesis. Generative adversarial networks (GANs) were used to synthesize face images with varying ages. Debayan et al. [11] proposed synthesizing a face image with a known identity at a specific age and then comparing it with a query image using a face verification scheme. Zhao et al. [52] proposed an end-to-end training architecture for face synthesis and recognition, while Huang et al. [22] proposed a multitask learning framework for face recognition, age classification, and face synthesis.

Age disentanglement. Another line of research focuses on modeling the face image embedding as a nonlinear combination of identity and age-related factors, and disentangling the two. Gong et al. [17] proposed a probabilistic model comprising a latent identity factor that is age-invariant and a latent age factor. The model was trained using expectation-maximization (EM). Gong et al. [18] later proposed an entropy maximization descriptor that proved to be more discriminative and resulted in improved verification accuracy using the age-invariant features. Wen et al. [48] suggested

a deep learning framework to learn the latent age factor, while SVM with a gradient orientation pyramid (GOP) was proposed by Ling et al. [27] to discard the age information from an image. In contrast to these works, which factorize the face image, our WMI-AI approach disentangles the age from identity features by learning a mutual representation that minimizes their mutual information while learning age-invariant face embeddings for recognition.

Discriminative convolutional neural networks. Recent research on age-invariant face verification has focused on improving the recognition models through discriminative approaches. Wang et al. [47] proposed the OE-CNN (Orthogonal-Embedding Convolutional Neural Network), which learns an orthogonal representation for the embedding of the face and age using angular and radial representations. Another approach, proposed by Wang et al. [44], uses a decorrelation method to decompose age and identity features through decorrelated adversarial learning (DAL). Lee et al. [26] proposed to improve verification results for child images using an inter-prototype loss function that minimizes the similarity of child images and resulted in improved verification accuracy of adult-child image pairs.

2.2 Mutual Information in Representation Learning

The use of mutual information (MI) in representation learning has gained increasing attention in recent years. Schwartz and Tishby [39] used MI to analyze the relationship between the different layers of a deep neural network (DNN). Later, Tishby and Zaslavsky [43] applied the bottleneck principle to optimize the size of the representation in a DNN through mutual information minimization. As MI is difficult to compute, researchers have focused on using convolutional neural networks (CNNs) to estimate it. Cheng et al. [9] proposed CLUB, which uses a CNN to estimate the MI between samples from an unknown distribution using a lower contrastive logarithmic ratio bound. Belghazi et al. [3] introduced MINE - mutual information neural estimation, which computes a lower bound of the MI using a critic DNN network, and showed it to be a tight bound in various cases, including domain adaptation.

Mutual information also plays a role in age-invariant face recognition models. Hou et al. [19] and Xie et al. [50] proposed to minimize MI between the age and identity components of a face image. These recent works mainly focus on using neural estimation for MI. In contrast, the proposed WMI-AI method minimizes the Wasserstein distance of the Jensen-Shannon divergence to minimize the MI between the age and identity embeddings.

2.3 Wasserstein Distance

The Wasserstein distance is a measure of the distance between two probability distributions and is widely used in the training of deep learning networks. This distance metric has been particularly effective in the field of generative adversarial networks (GANs), where it has helped stabilize adversarial training [1]. Shen et al. [38] suggested the WD-GRL Wasserstein Distance Guided Representation Learning for domain adaptation applications, by estimating and minimizing the cross-domain Wasserstein distance. The Wasserstein distance has also been applied to a range of

computer vision and machine learning tasks, including object detection [51], scene classification [15], and multi-source domain adaptation [49] to name a few. In contrast, our approach involves the reduction of mutual information between age and identity embeddings by minimizing the Wasserstein distance. This aligns with our objective of disentangling these attributes to enhance the accuracy of face verification in the proposed WMI-AI scheme, particularly when analyzing face images that exhibit notable age discrepancies.

3 AGE-INVARIANT FACE EMBEDDING

In this work, we propose to train an age-invariant face embedding for face verification. We propose to disentangle the age and identity attributes in a high-dimensional embedding space by minimizing the Jensen-Shannon Divergence (JSD) between the identity and age embeddings, while jointly optimizing the embeddings for face recognition and age estimation. In line with Fig. 2, the proposed method consists of two components: computing the face image embeddings for age and identity, and a mutual information discriminator. Given a face image x , we train the age and identity embeddings, consisting of an identity CNN backbone and encoder f_{id} and an age CNN and encoder f_a , respectively. The identity encoder outputs the embedding \hat{x}_{id} , which is passed through the identity classifier g_{id} . Similarly, the age encoder outputs the embedding \hat{x}_a , which is then passed through a regression layer g_a to predict the face image age. The face and age encoders are detailed in Section 3.2. The MI discriminator D is used to classify whether the mutual representation \hat{x}_{id}, \hat{x}_a is drawn from the mutual probability $\mathbb{P}(\hat{x}_{id}, \hat{x}_a)$ or from the independent probabilities $\mathbb{P}(\hat{x}_{id}, \hat{x}_a) = \mathbb{P}(\hat{x}_{id})\mathbb{P}(\hat{x}_a)$. The discriminator and its objective are detailed in Section 3.1.

We train the embedding \hat{x}_{id} adversarially with the discriminator loss, to fool the discriminator to predict that \hat{x}_{id} and \hat{x}_a were drawn from an independent distribution. However, adversarial training is known to be unstable and difficult to converge, so we propose training the discriminator using the Wasserstein distance cost, which was shown to improve the convergence of adversarial training [1]. The multitask training and optimization are described in Section 3.3. Lastly, we discuss in Section 3.4 the use of a pretrained age estimation network when the age labels of the training set are unknown.

3.1 Discriminator Architecture and Training Method

We represent the mutual embedding of age $\hat{x}_a \in \mathbb{R}^{d_a}$ and identity $\hat{x}_{id} \in \mathbb{R}^{d_{id}}$ as the random variable $\hat{x} \triangleq (\hat{x}_{id}, \hat{x}_a) \in \mathbb{R}^{d_{id}+d_a}$. Let z be a binary random variable

$$\hat{x} \sim \begin{cases} \mathbb{P}(\hat{x}_{id}, \hat{x}_a), & \text{for } z = 0 \\ \mathbb{P}(\hat{x}_{id})\mathbb{P}(\hat{x}_a), & \text{for } z = 1 \end{cases}. \quad (1)$$

The mutual information between \hat{x} and z can be expressed as:

$$I(\hat{x}; z) = JSD(\mathbb{P}(\hat{x}_{id}, \hat{x}_a) \parallel \mathbb{P}(\hat{x}_{id})\mathbb{P}(\hat{x}_a)) \quad (2)$$

where JSD is the Jensen-Shannon Divergence. The objective of the discriminator D is to distinguish between the two representations in Eq. 1 and estimate the random variable z .

Hence, the objective of D is to maximize the JSD , while our adversarial-training objective is to minimize the JSD with respect to \hat{x}_{id} , given \hat{x}_a . The discriminator loss function is thus given by:

$$L_d(\hat{x}) = \frac{1}{2}E_{\hat{x} \sim \mathbb{P}(\hat{x}_{id}, \hat{x}_a)} \log(1-D(\hat{x})) + \frac{1}{2}E_{\hat{x} \sim \mathbb{P}(\hat{x}_{id})\mathbb{P}(\hat{x}_a)} \log D(\hat{x}). \quad (3)$$

Minimizing the JSD between the distributions $\mathbb{P}(\hat{x}_{id}, \hat{x}_a)$ and $\mathbb{P}(\hat{x}_{id})\mathbb{P}(\hat{x}_a)$ is equivalent to minimizing the MI between \hat{x}_{id} and \hat{x}_a . Thus, adversarial training of the embedding \hat{x}_{id} to minimize the JSD will result in age-invariant embeddings.

To draw samples from the mutual embedding $\mathbb{P}(\hat{x}_{id}, \hat{x}_a)$, we follow Chen et al. [8] and combine the embeddings \hat{x}_{id} and \hat{x}_a into a single embedding \hat{x} . To create samples from the statistically independent embeddings $\mathbb{P}(\hat{x}_{id})\mathbb{P}(\hat{x}_a)$, we combine the embeddings \hat{x}_{id} and \hat{x}_a of *different* images. These are known not to be statistically independent, and we label the result \bar{x} . Training a discriminator using the JSD loss in Eq. 3 might lead to convergence issues [25]. For that, we construct a Wasserstein distance discriminator [38], which utilizes a critic network (MLP) trained with a Wasserstein distance and a gradient penalty term. The architecture of the critic layer is detailed in Table 1 of the Appendix, and the training loss of the discriminator is given by

$$L_w(\mathbb{P}_M, \mathbb{P}_I) = \sup_{f_w} E_{\hat{x} \sim \mathbb{P}_M} [f_w(\hat{x})] - E_{x \sim \mathbb{P}_I} [f_w(\hat{x})]. \quad (4)$$

For the sake of brevity, let $\mathbb{P}(\hat{x}_{id}, \hat{x}_a) = \mathbb{P}_M$ and $\mathbb{P}(\hat{x}_{id})\mathbb{P}(\hat{x}_a) = \mathbb{P}_I$. The critic network f_w is trained to maximize the Wasserstein distance between \mathbb{P}_M and \mathbb{P}_I [1], and the Wasserstein distance in Eq. 4 is approximated by training the critic network D to maximize

$$L_w(\mathbb{P}_M, \mathbb{P}_I) = \frac{1}{|\mathbb{P}_M|} \sum_{\hat{x} \in \mathbb{P}_M} f_w(\hat{x}) - \frac{1}{|\mathbb{P}_I|} \sum_{\bar{x} \in \mathbb{P}_I} f_w(\bar{x}). \quad (5)$$

To maintain the Lipschitz constraint of the Wasserstein distance and improve the stability of the training process of the critic network, we incorporate a gradient penalty term [38]. The critic network D and adversarial encoder f_{id} are trained in two stages: first, we freeze f_{id} and f_a and optimize the critic network D to maximize the Wasserstein distance. We then freeze the critic network and optimize the f_{id} and f_a networks to minimize the Wasserstein distance and the JSD . The overall optimization is thus given by

$$L = \min_{f_{id}, f_a} \max_{\mathbf{D}} (L_w - \lambda_g L_{grad}), \quad (6)$$

where L_{grad} is the gradient penalty term and we set $\lambda_g = 10$ in line with [1],[38], where a thorough ablation study of λ_g was conducted.

3.2 Face and Age Encoder Architecture

The backbone architecture and losses for face recognition and age estimation were adopted from the ArcFace network [13]. Thus, we used the Resnet101 backbone for the identity encoder and the Resnet50 network for the age encoder. For the age estimation network g_a , following Rothe et al. [36], we use a single fully connected layer, which takes as input the normalized age embedding \hat{x}_a and is trained using a discrete classification loss L_a . The identity prediction network g_{id} ,

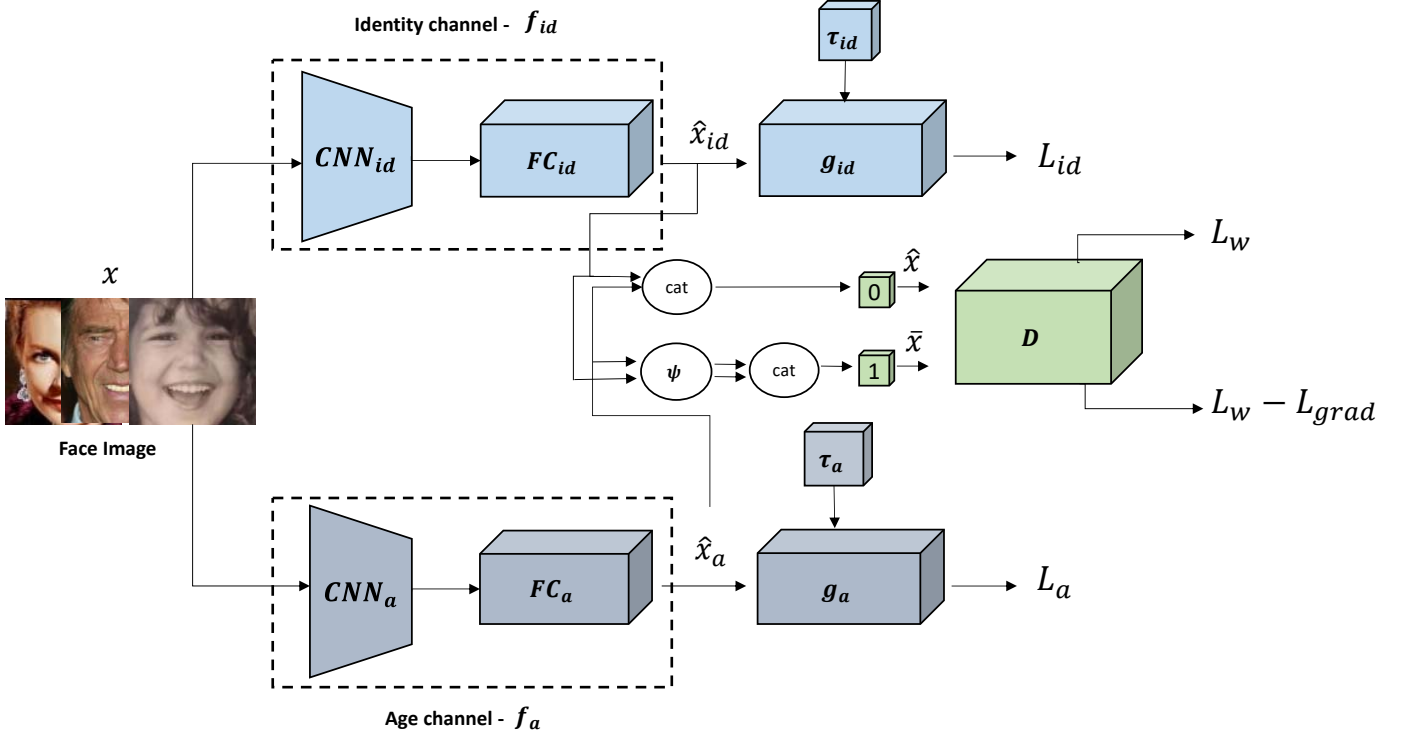


Fig. 2: The proposed network involves an identity encoder network f_{id} and an age encoder f_a . When given a facial image x , f_{id} generates the identity embedding \hat{x}_{id} , while f_a computes the age embedding \hat{x}_a . These encoders are optimized for facial recognition and age estimation using the classifiers g_{id} and g_a . During adversarial training, the discriminator D utilizes the embedding pairs $\hat{x} = (\hat{x}_{id}^i, \hat{x}_a^i)$ and randomly shuffled embedding pairs $\bar{x} = (\hat{x}_{id}^i, \hat{x}_a^j)$, $i \neq j$, as positive and negative samples, correspondingly.

also uses a single fully connected layer, given the identity embedding \hat{x}_{id} , and is trained using the ArcFace loss [13] L_{id} .

3.3 Multitask Training

The embedding encoders and discriminator are jointly trained in an adversarial manner, to compute embeddings that are not discriminative with respect to age, while the discriminator is trained to distinguish between age-invariant and age-dependent embeddings. Through this adversarial training, the MI between the age and identity representations is minimized, and the resulting identity embeddings are made age-invariant. Our architecture is trained as a multitask optimization using a min-max term for the discriminator. We suggest a four-step training:

- 1) Forward pass the image x through the encoders to compute \hat{x}_{id} and \hat{x}_a .
- 2) Freeze f_{id} and f_a and using \hat{x}_{id}, \hat{x}_a , train the discriminator and the critic network D by maximizing the loss in Eq. 6.
- 3) Freeze f_a and forward pass \hat{x}_{id}, \hat{x}_a to compute the Wasserstein distance using the trained discriminator and obtain $L_w(\hat{x}_{id}, \hat{x}_a)$.
- 4) To optimize f_{id} , first compute L_a and L_{id} following Section 3.2. Then, minimize L_{id} and L_w . To optimize f_a , minimize L_a

Thus, the overall training loss is

$$L = L_{id}(\hat{x}_{id}) + \lambda_w L_w(\hat{x}_{id}, \hat{x}_a) + \lambda_a L_a(\hat{x}_a), \quad (7)$$

where λ_w and λ_a are hyperparameters. The ablation of λ_w is studied in Section 4.3 where we show $\lambda_w = 0.1$ to be optimal in terms of verification accuracy. As for λ_a , since we freeze the age embedding network f_a while optimizing the Wasserstein distance loss L_w , the accuracy of our WMI-AI approach is invariant to λ_a , and we set $\lambda_a = 1$. The training is summarized in Algorithm 1 in the Appendix.

3.4 Using a Pretrained Age Estimator

In many situations, the age labels of the face images are unknown. Hence, a pre-trained age estimation model is utilized to compute the age embeddings \hat{x}_a , while the identity embeddings \hat{x}_{id} are computed the same as in the supervised case in Section 3.3. We use two training datasets: the first has both identity and age labels, while the second lacks age labels. For the second dataset, the pretrained age estimation network trained on the first dataset is used to obtain the age embeddings. During training, only the face recognition task is trained, while \hat{x}_a remains fixed for all images. The Wasserstein discriminator has the same task as in the supervised case, minimizing the MI between \hat{x}_{id} and the fixed age embedding \hat{x}_a . This architecture is shown in Fig. 2. The training loss consists of the Wasserstein discriminator and the identity recognition losses,

$$L = L_{id}(\hat{x}_{id}) + \lambda_w L_w(\hat{x}_{id}, \hat{x}_a) \quad (8)$$

where λ_w is a hyperparameter (See Section 4.3).

4 EXPERIMENTAL RESULTS

4.1 Training details

Training Parameters: The proposed scheme was trained using a batch size of 1,024 with gradient accumulation to account for the limited GPU memory. We used the SGD optimizer with a momentum value of 0.9 and a weight decay of $5 \cdot 10^{-4}$ for the identity channel, g_{id} and f_{id} , as well as for the age channel, g_a and f_a . The initial learning rate was set at $\lambda = 0.1$ for the identity channel and $\lambda = 10^{-2}$ for the age channel, with both values decaying to 0 during training. The discriminator was optimized using the RMS prop optimizer with a fixed learning rate of $\lambda = 10^{-4}$, $\alpha=0.99$, and $\varepsilon = 10^{-8}$, without momentum. The frequency of discriminator optimization was set at 50, such that for each backbone optimization step, the discriminator was optimized by 50 steps. The hyperparameters were initialized to $\lambda_w = 0.1$, $\lambda_{id} = 1$, $\lambda_g = 1$, and $\lambda_a = 0.25$, respectively. The training process was conducted using two Nvidia V100 GPUs, each with 32GB memory.

Training dataset: As a training dataset we used a clean version of the widely used MS-Celeb-1M (MS1M) face verification dataset. MS1M consists of 1M identities and more than 10M images. Deng et al. [13] suggested using a clean version of MS1M called MS1MV2, which contains 5.7M images and 85K identities. This MS1M version has been widely used in face recognition to achieve state-of-the-art results on multiple benchmarks. Deng et al. [13] also suggested a clean version of MS1M called MS1MV3, which is an extended version of MS1MV2 that includes 93K identities and 5.1M images. The images in MS1MV3 were manually labeled and aligned using 5 facial landmarks using RetinaFace [14]. We trained our architecture using MS1MV2 and MS1MV3, where all images were aligned, cropped to a size of 112×112 , and normalized to a dynamic range of $[-1, 1]$. During training, the images were augmented using random horizontal flipping.

4.2 Cross-Age Datasets

Our proposed method was evaluated on various cross-age datasets, including CALFW [53], AgeDB-30 [31], CACD-VS [6], and ECAF [22]. Qualitative verification results from each dataset are presented in Fig. 3. These datasets contain images with a significant age gaps, with the ECAF (adult, child) dataset having an average age gap of 41 years. The images are captured “in the wild” in different scenarios, featuring diverse poses, lighting conditions, and facial expressions, some available in either black-and-white or color.

CALFW: The Cross-Age Labeled Faces in the Wild (CALFW) dataset [53] is a subset of the Labeled Faces in the Wild (LFW) dataset [20]. The CALFW dataset consists of 13,216 images of 574 individuals, with ages ranging from 0 to 100 years. The dataset has 3,000 positive pairs of images with large age gaps, the evaluation protocol uses 10 folds of verification, each fold consisting of 600 positive and negative pairs. We follow this protocol to evaluate our method, and the results are summarized in Table 1. All of the verification results in Table 1 are cited from the corresponding papers, except for the ArcFace [12] results using the MS1MV3 dataset which was computed

with the publicly available ArcFace code¹. Two versions of our proposed WMI-AI scheme were trained using either the MS1MV2 or MS1MV3 datasets separately. In both cases, we observed an accuracy improvement of 0.06% and 0.02%, respectively, compared to the SOTA. In particular, when training with the MS1MV3 dataset, the verification accuracy improved consistently between different methods.

AgeDB-30: The AgeDB dataset [31] contains 16,488 images of 568 identities that were manually annotated and labeled. Four protocols for age-variant face verification are used with this dataset, where each protocol is subject to a different age gap. AgeDB-30, a subset of the AgeDB dataset, is the most challenging protocol with a 30-year age gap between the corresponding image pairs. In total, AgeDB-30 has 6K pairs divided into 10-fold verification sets. The evaluation results are summarized in Table 2, where all of the results are cited from the corresponding papers. The results show that our approach achieves an incremental improvement compared to the state-of-the-art results for both training datasets, as in the case of the CALFW data set, the training results on the cleaned MS1MV3 dataset outperform those of the MS1MV2 dataset.

CACD-VS: Cross-Age Celebrity Dataset - Verification Subset [6] is a subset of the larger CACD dataset [7], consisting of 163,446 images of 2,000 celebrities. The CACD-VS subset is manually sampled and annotated and contains 4K pairs of positive and negative face images. The face verification protocol is similar to LFW and the results are summarized in Table 3. Except for the verification outcomes of ArcFace [12] on the MS1MV3 dataset, which were computed using the publicly accessible ArcFace code, the verification results were obtained from their respective papers. The results show that the proposed WMI-AI achieves 99.57% accuracy, outperforming the previous state-of-the-art methods such as MTLFACE [22] and ArcFace [12]. The WMI-AI accuracy is consistently high across both training datasets, confirming the effectiveness of our approach in minimizing the intraclass age-related variations.

ECAF Dataset: The ECAF (Evaluation of Cross-Age Face) dataset [22] is a recent face recognition dataset introduced by Haung et al. [22] that comprises a diverse range of ages, from children to adults. It consists of two subsets, ECAF-AdultChild and ECAF-ChildChild, of adult-child and child-child face image pairs. The ECAF is the largest cross-age dataset with an average age difference of 41 years, consisting of 5,265 images from 613 identities, resulting in 6K (Adult, Child) and 4K (Child, Child) image pairs. In this study, we adopt the evaluation protocol utilized in LFW and assess the performance of our network using the MS1MV2 dataset since there are no previous results reported for the MS1MV3 dataset. Our evaluation results are reported in Table 4, where the results are cited from the respective papers. The proposed WMI-AI approach shows significant improvements in the verification results on the challenging ECAF dataset, with an average accuracy increase of 3.18% for the (Adult, Child) pairs and 3.24% for the (Child, Child) pairs compared to the current state-of-the-art result. These results exemplify the effectiveness of our approach in handling large age differences between images, as well as

1. <https://github.com/deepinsight/insightface>

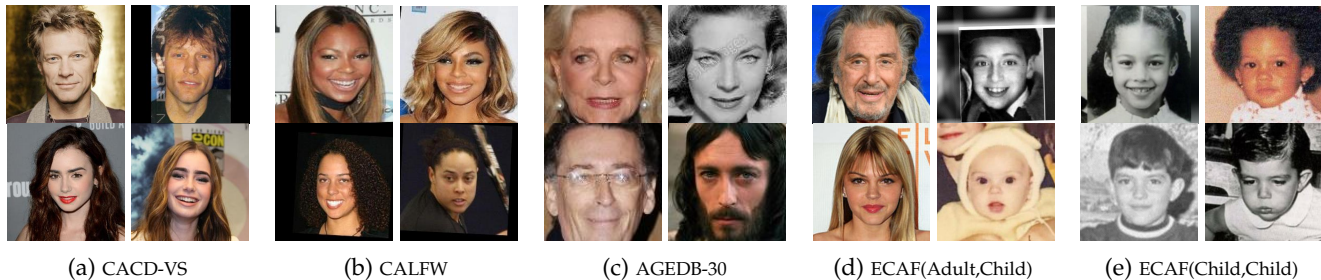


Fig. 3: Qualitative face verification results using different image datasets. The first row shows true positive verification results, while, the second row shows false negative verification results.

TABLE 1: Face verification results evaluated using the CALFW dataset [53]. The leading results are highlighted in **bold**.

Method	Dataset	Accuracy[%]
MTLFace[22]		95.62
Arc-DiscFace[24]		96.15
ElasticFace[4]		96.18
ArcFace[12]	MS1MV2	96.18
CosFace[13]		96.20
CurricularFace[21]		96.20
WMI-AI (ours)		96.26
Implicit[50]		95.82
DPNN[10]	MS1MV3	96.23
ArcFace[12]		96.26
WMI-AI (ours)		96.28

TABLE 3: Face verification results evaluated using the CACD-VS dataset [6]. The leading results are highlighted in **bold**.

Method	Dataset	Accuracy [%]
MTLFACE[22]		99.55
ArcFace[12]	MS1MV2	99.55
WMI-AI (ours)		99.57
ArcFace[12]		99.55
Implicit[50]	MS1MV3	99.57
WMI-AI (ours)		99.57

achieving age-invariant representations, thus improving the face verification accuracy.

4.3 Ablation Study

We examined the impact of the discriminator architectures, as well as the effect of the weight of the discriminator loss λ_w , in Eq. 7, with respect to the other training losses. We tested the performance of our approach with different values of λ_w in Table 5, including $\lambda_w = 0$ that corresponds to training our WMI-AI approach without disentanglement. $\lambda_w = 0.1$ achieves the highest verification accuracy, showing a “sweetspot” effect, where using a higher or lower λ_w reduces the accuracy.

We also evaluated the use of the proposed disentanglement on the Jensen-Shannon divergence (JSD), which measures the MI between age and identity embeddings. The results for minimizing the JSD when training the proposed

TABLE 2: Face verification results evaluated using the AGEDB-30 dataset [31]. The leading results are highlighted in **bold**.

Method	Dataset	Accuracy[%]
MTLFACE[31]		96.23
CosFace[13]		98.07
MagFace[29]		98.17
ArcFace[12]	MS1MV2	98.2
CurricularFace[21]		98.32
Arc-DiscFace[24]		98.35
ElasticFace[4]		98.35
WMI-AI (ours)		98.37
Implicit[50]		95.82
DPNN[10]	MS1MV3	98.47
ArcFace[12]		98.55
WMI-AI (ours)		98.57

TABLE 4: Face verification results evaluated using the ECAF dataset [22]. The leading results are highlighted in **bold**.

Method	(Adult, ,Child)	(Child ,Child)
Human, Average[22]	73.34	68.62
Human, Voting[22]	85.95	78.75
Softmax[22]	85.03	88.25
CosFace[13]	85.72	90.75
ArcFace[12]	86.52	90.65
CurricularFace[21]	84.78	90.80
MTLFace[22]	87.55	91.20
WMI-AI (ours)	90.73	94.44

network with ($\lambda_w = 0.1$) and without ($\lambda_w = 0$) disentanglement using the MS1MV2 and MS1MV3 datasets are shown in Fig. 4. The proposed scheme better minimized the MI in both cases. It is interesting to note that applying our network without the disentanglement ($\lambda_w = 0$) also reduces the JSD, as the identity and age encoders f_{id} and f_a , respectively, compute identity-specific and age-specific embeddings, thus increasing the JSD between them. However, applying the proposed disentanglement is shown to better disentangle these embeddings statistically.

An Ablation of the WMI backbone and critic network is reported in Table 2 of the Appendix.

5 CONCLUSIONS AND FUTURE WORK

This paper proposes a new approach to age-invariant face embedding based on the Wasserstein distance. Our approach disentangles age and identity embeddings of face images,

TABLE 5: Ablation study of the verification accuracy results [%] on the cross-age datasets with respect to λ_w .

	λ_w	CALFW	AGEDB30	CACD-VS	ECAF(A,C)	ECAF(C,C)
MS1MV2	0	96.18	98.20	95.55	90.43	94.00
	0.1	96.26	98.37	99.57	90.73	94.40
	1.0	96.21	98.28	99.57	90.41	94.20
	2.0	96.15	98.20	99.55	89.80	94.10
MS1MV3	0	96.26	98.55	99.55	92.35	95.05
	0.1	96.28	98.57	99.57	92.70	95.20
	1.0	96.25	98.47	99.55	91.60	94.70
	2.0	96.18	98.20	99.50	91.55	94.50

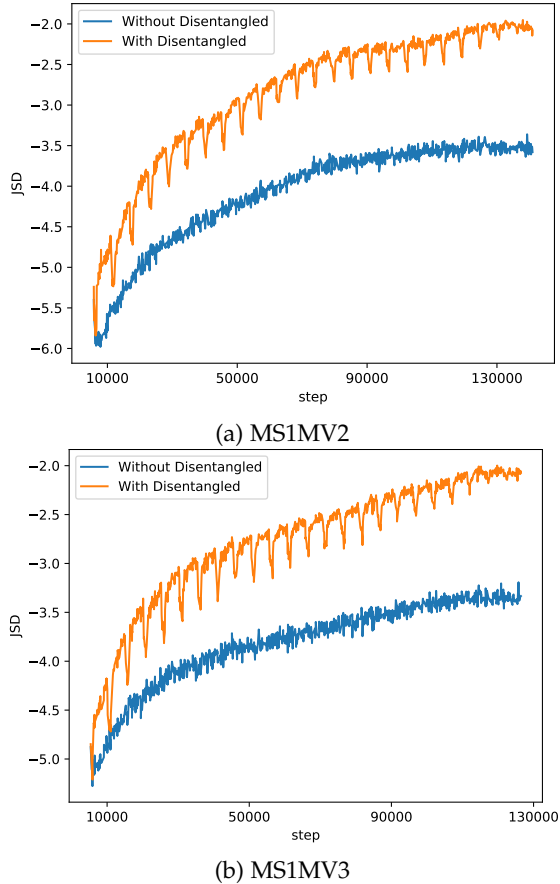


Fig. 4: The Jensen-Shannon divergence (JSD) with ($\lambda_w = 0.1$) and without ($\lambda_w = 0$) disentanglement when trained using the MS1MV2 and MS1MV3 datasets. We report the JSD with respect to the optimization steps of our scheme.

enabling improved face verification performance in age-variant datasets. We apply multitask training with a Wasserstein distance discriminator that minimizes the MI between age and identity embeddings by minimizing the Jensen-Shannon divergence. Our experimental results demonstrate the effectiveness of the proposed method, with superior face verification accuracy compared to state-of-the-art methods on multiple contemporary age-variant face datasets. Thus, we believe that the proposed WMI-AI method offers a promising solution to face verification in datasets with significant age-varying images of the same subjects. Future work could study the applicability of our approach to domains beyond face verification, such as kinship verification, where age variance plays a significant role in identifying family-related

face image pairs.

REFERENCES

- [1] Martin Arjovsky, Soumith Chintala, and Léon Bottou. Wasserstein generative adversarial networks. In *Proceedings of the International Conference on Machine Learning (ICML)*, pages 214–223. PMLR, 2017.
- [2] Joe Bathelt, P. Cédric Koolschijn, and Hilde M Geurts. Age-variant and age-invariant features of functional brain organization in middle-aged and older autistic adults. *Aging Ment Health*, 11(1), 2020.
- [3] Mohamed Ishmael Belghazi, Aristide Baratin, Sai Rajeshwar, Sherjil Ozair, Yoshua Bengio, Aaron Courville, and Devon Hjelm. Mutual information neural estimation. In *Proceedings of the International Conference on Machine Learning (ICML)*, pages 531–540. PMLR, 2018.
- [4] Fadi Boutros, Naser Damer, Florian Kirchbuchner, and Arjan Kuijper. ElasticFace: elastic margin loss for deep face recognition. In *Proceedings of the IEEE Conference on Computer Vision and Pattern Recognition Workshops (CVPRW)*, pages 1577–1586, 2022.
- [5] Praveen Kumar Chandaliya and Neeta Nain. Childgan: Face aging and rejuvenation to find missing children. *Pattern Recognition*, 129:108761, 2022.
- [6] Bor-Chun Chen, Chu-Song Chen, and Winston H. Hsu. Cross-age reference coding for age-invariant face recognition and retrieval. In *Proceedings of the European Conference on Computer Vision (ECCV)*, 2014.
- [7] Bor-Chun Chen, Chu-Song Chen, and Winston H. Hsu. Cross-age reference coding for age-invariant face recognition and retrieval. In *Proceedings of the European Conference on Computer Vision (ECCV)*, 2014.
- [8] Xi Chen, Yan Duan, Rein Houthoofd, John Schulman, Ilya Sutskever, and Pieter Abbeel. InfoGAN: interpretable representation learning by information maximizing generative adversarial nets. In *Neural Information Processing Systems (NeurIPS)*, NIPS’16, page 2180–2188, 2016.
- [9] Pengyu Cheng, Weituo Hao, Shuyang Dai, Jiachang Liu, Zhe Gan, and Lawrence Carin. Club: A contrastive log-ratio upper bound of mutual information. In *Proceedings of the International Conference on Machine Learning (ICML)*, pages 1779–1788. PMLR, 2020.
- [10] Grigorios G. Chrysos, Stylianos Moschoglou, Giorgos Bouritsas, Jiankang Deng, Yannis Panagakis, and Stefanos P Zafeiriou. Deep polynomial neural networks. *IEEE Transactions on Pattern Analysis and Machine Intelligence (PAMI)*, pages 1–1, 2021.
- [11] Debayan Deb, Divyansh Aggarwal, and Anil K. Jain. Identifying missing children: Face age-progression via deep feature aging. In *Proceedings of the International Conference on Pattern Recognition (ICPR)*, pages 10540–10547, 2021.
- [12] Jiankang Deng, Jia Guo, Tongliang Liu, Mingming Gong, and Stefanos Zafeiriou. Sub-center ArcFace: boosting face recognition by large-scale noisy web faces. In *Proceedings of the European Conference on Computer Vision (ECCV)*, 2020.
- [13] Jiankang Deng, Jia Guo, Xue Niannan, and Stefanos Zafeiriou. ArcFace: additive angular margin loss for deep face recognition. In *Proceedings of the IEEE Conference on Computer Vision and Pattern Recognition (CVPR)*, 2019.
- [14] Jiankang Deng, Jia Guo, Evangelos Ververas, Irene Kotsia, and Stefanos Zafeiriou. RetinaFace: single-shot multi-level face localisation in the wild. In *Proceedings of the IEEE Conference on Computer Vision and Pattern Recognition (CVPR)*, June 2020.

- [15] Konstantinos Drossos, Paul Magron, and Tuomas Virtanen. Unsupervised adversarial domain adaptation based on the wasserstein distance for acoustic scene classification. In *Proceedings of the IEEE Workshop on Applications of Signal Processing to Audio and Acoustics*, pages 259–263. IEEE, 2019.
- [16] Shai Gepshtein and Yosi Keller. Iterative spectral independent component analysis. *Signal Processing*, 155:368–376, 2019.
- [17] Dihong Gong, Zhifeng Li, Dahua Lin, Jianzhuang Liu, and Xiaoou Tang. Hidden factor analysis for age invariant face recognition. In *Proceedings of the IEEE Conference on Computer Vision and Pattern Recognition (CVPR)*, pages 2872–2879, 2013.
- [18] Dihong Gong, Zhifeng Li, Dacheng Tao, Jianzhuang Liu, and Xuelong Li. A maximum entropy feature descriptor for age invariant face recognition. In *Proceedings of the IEEE Conference on Computer Vision and Pattern Recognition (CVPR)*, pages 5289–5297, 2015.
- [19] Xuege Hou, Yali Li, and Shengjin Wang. Disentangled representation for age-invariant face recognition: A mutual information minimization perspective. In *Proceedings of the IEEE Conference on Computer Vision and Pattern Recognition (CVPR)*, pages 3692–3701, 2021.
- [20] Gary B. Huang, Manu Ramesh, Tamara Berg, and Erik Learned-Miller. Labeled faces in the wild: A database for studying face recognition in unconstrained environments. Technical Report 07-49, University of Massachusetts, Amherst, October 2007.
- [21] Yuge Huang, Yuhan Wang, Ying Tai, Xiaoming Liu, Pengcheng Shen, Shaoxin Li, and Feiyue Huang Jilin Li. CurricularFace: adaptive curriculum learning loss for deep face recognition. In *Proceedings of the IEEE Conference on Computer Vision and Pattern Recognition (CVPR)*, June 2020.
- [22] Zhizhong Huang, Junping Zhang, and Hongming Shan. When age-invariant face recognition meets face age synthesis: A multi-task learning framework. In *Proceedings of the IEEE Conference on Computer Vision and Pattern Recognition (CVPR)*, 2021.
- [23] A. Hyvarinen. Fast and robust fixed-point algorithms for independent component analysis. *IEEE Transactions on Neural Networks*, 10(3):626–634, 1999.
- [24] Insoo Kim, Seungju Han, Seong-Jin Park, Ji-won Baek, Jinwoo Shin, Jae-Joon Han, and Changkyu Choi. DiscFace: minimum discrepancy learning for deep face recognition. In Hiroshi Ishikawa, Cheng-Lin Liu, Tomas Pajdla, and Jianbo Shi, editors, *Proceedings of the Asian Conference on Computer Vision (ACCV)*, pages 358–374, 2021.
- [25] Naveen Kodali, Jacob Abernethy, James Hays, and Zsolt Kira. On convergence and stability of GANs. *arXiv preprint arXiv:1705.07215*, 2017.
- [26] Jungsoo Lee, Jooyeol Yun, Sunghyun Park, Yonggyu Kim, and Jaegul Choo. Improving face recognition with large age gaps by learning to distinguish children. In *Proceedings of the British Machine Vision Conference (BMVC)*, 2021.
- [27] Haibin Ling, Stefano Soatto, Narayanan Ramanathan, and David W. Jacobs. Face verification across age progression using discriminative methods. *IEEE Transactions on Information Forensics and Security*, 5(1):82–91, 2010.
- [28] Fan Liu, Zewen Li, Wenjie Yang, and Feng Xu. Age-invariant adversarial feature learning for kinship verification. *Mathematics*, 10(3), 2022.
- [29] Qiang Meng, Shichao Zhao, Zhida Huang, and Feng Zhou. Mag-Face: A universal representation for face recognition and quality assessment. In *Proceedings of the IEEE Conference on Computer Vision and Pattern Recognition (CVPR)*, 2021.
- [30] Dario Moreno-Agostino, Alejandro de la Torre-Luque, Leandro da Silva-Sauer, Bruce W Smith, and Bernardino Fernández-Calvo. The age-invariant role of resilience resources in emotional symptomatology. *Molecular Autism*, 26(1), 2022.
- [31] Stylianos Moschoglou, Athanasios Papaioannou, Christos Sagonas, Jiankang Deng, Irene Kotsia, and Stefanos Zafeiriou. Agedb: the first manually collected, in-the-wild age database. In *Proceedings of the IEEE Conference on Computer Vision and Pattern Recognition Workshops (CVPRW)*, volume 2, page 5, 2017.
- [32] W. Ouyang, X. Wang, X. Zeng, Shi Qiu, P. Luo, Y. Tian, H. Li, Shuo Yang, Zhe Wang, Chen-Change Loy, and X. Tang. DeepID-Net: deformable deep convolutional neural networks for object detection. In *Proceedings of the IEEE Conference on Computer Vision and Pattern Recognition (CVPR)*, pages 2403–2412, jun 2015.
- [33] Unsang Park, Yiyang Tong, and Anil K. Jain. Age-invariant face recognition. *IEEE Transactions on Pattern Analysis and Machine Intelligence (PAMI)*, 32(5):947–954, 2010.
- [34] Narayanan Ramanathan and Rama Chellappa. Modeling shape and textural variations in aging faces. In *Proceedings of the IEEE International Conference on Automatic Face and Gesture Recognition*, pages 1–8, 2008.
- [35] Joseph P Robinson, Ming Shao, Yue Wu, and Yun Fu. Families in the wild (FIW): Large-scale kinship image database and benchmarks. In *Proceedings of the ACM International Conference on Multimedia*, pages 242–246. ACM, 2016.
- [36] Rasmus Rothe, Radu Timofte, and Luc Van Gool. DEX: deep expectation of apparent age from a single image. In *Proceedings of the International Conference on Computer Vision Workshops (ICCVW)*, pages 252–257, 2015.
- [37] Muhammad Sajid, Tamoor Shafique, Sohaib Manzoor, Faisal Iqbal, Hassan Talal, Usama Samad Qureshi, and Imran Riaz. Demographic-assisted age-invariant face recognition and retrieval. *Symmetry*, 10(5), 2018.
- [38] Jian Shen, Yanru Qu, Weinan Zhang, and Yong Yu. Wasserstein distance guided representation learning for domain adaptation. In *Proceedings of the AAAI Conference on Artificial Intelligence (AAAI)*, AAAI’18/IAAI’18/EAAI’18, 2018.
- [39] Ravid Shwartz-Ziv and Naftali Tishby. Opening the black box of deep neural networks via information. *CoRR*, abs/1703.00810, 2017.
- [40] Yu Su, Shiguang Shan, Xilin Chen, and Wen Gao. Hierarchical ensemble of global and local classifiers for face recognition. *IEEE Transactions on Image Processing*, 18(8):1885–1896, 2009.
- [41] S. N. Sujay, H. S. Manjunatha Reddy, and J. Ravi. Face recognition using extended lbp features and multilevel svm classifier. In *Proceedings of the IEEE International Conference on Electrical, Electronics, Communication, Computer, and Optimization Techniques*, pages 1–4, 2017.
- [42] Yaniv Taigman, Ming Yang, Marc’Aurelio Ranzato, and Lior Wolf. DeepFace: closing the gap to human-level performance in face verification. In *Proceedings of the IEEE Conference on Computer Vision and Pattern Recognition (CVPR)*, pages 1701–1708, 2014.
- [43] Naftali Tishby and Noga Zaslavsky. Deep learning and the information bottleneck principle. In *Proceedings of the IEEE Information Theory Workshop*, pages 1–5, 2015.
- [44] Hao Wang, Dihong Gong, Zhifeng Li, and Wei Liu. Decorrelated adversarial learning for age-invariant face recognition. In *Proceedings of the IEEE Conference on Computer Vision and Pattern Recognition (CVPR)*, pages 3522–3531, 2019.
- [45] Hao Wang, Yitong Wang, Zheng Zhou, Xing Ji, Dihong Gong, Jingchao Zhou, Zhifeng Li, and Wei Liu. CosFace: Large margin cosine loss for deep face recognition. In *Proceedings of the IEEE Conference on Computer Vision and Pattern Recognition (CVPR)*, pages 5265–5274, 2018.
- [46] Shuyang Wang, Zhengming Ding, and Yun Fu. Cross-generation kinship verification with sparse discriminative metric. *IEEE Transactions on Pattern Analysis and Machine Intelligence (PAMI)*, 41(11):2783–2790, 2019.
- [47] Yitong Wang, Dihong Gong, Zheng Zhou, Xing Ji, Hao Wang, Zhifeng Li, Wei Liu, and Tong Zhang. Orthogonal deep features decomposition for age-invariant face recognition. In Vittorio Ferrari, Martial Hebert, Cristian Sminchisescu, and Yair Weiss, editors, *Proceedings of the European Conference on Computer Vision (ECCV)*, pages 764–779, 2008.
- [48] Yandong Wen, Zhifeng Li, and Yu Qiao. Latent factor guided convolutional neural networks for age-invariant face recognition. In *Proceedings of the IEEE Conference on Computer Vision and Pattern Recognition (CVPR)*, pages 4893–4901, 2016.
- [49] Hanrui Wu, Yuguang Yan, Michael K Ng, and Qingyao Wu. Domain-attention conditional wasserstein distance for multi-source domain adaptation. *ACM Transactions on Intelligent Systems and Technology*, 11(4):1–19, 2020.
- [50] Jiu-Cheng Xie, Chi-Man Pun, and Kin-Man Lam. Implicit and explicit feature purification for age-invariant facial representation learning. *IEEE Transactions on Information Forensics and Security*, 17:399–412, 2022.
- [51] Pengcheng Xu, Prudhvi Gurram, Gene T. Whipples, and Rama Chellappa. Wasserstein distance based domain adaptation for object detection. *CoRR*, abs/1909.08675, 2019.
- [52] Jian Zhao, Shuicheng Yan, and Jiashi Feng. Towards age-invariant face recognition. *IEEE Transactions on Pattern Analysis and Machine Intelligence (PAMI)*, 44(1):474–487, 2022.

Appendix: Age-Invariant Face Embedding using the Wasserstein Distance



Fig. 1: From child to adult - the aging effect in face images. The images were taken from the ECAF dataset [2].

TABLE 1: The architecture of the age and identity classifiers, g_a and g_{id} , respectively, detailed in Section 3.2, and the critic network of the discriminator D as in Section 3.1.

g_{id}	g_a	D
Linear(emb, D_{cls})	Linear($emb, 101$)	Linear($emb \times 2, 150$) LeakyRelu($2 \cdot 10^{-1}$)
softmax	softmax	Linear($150, 60$) LeakyRelu($2 \cdot 10^{-1}$)
ArcFace Loss[1]	CE Loss	Linear($60, 20$) LeakyRelu($2 \cdot 10^{-1}$) Linear($20, 1$) BCE LOSS

An ablation of the identity channel backbone and the critic network is reported in Table 2. For that, we used the MS1MV2 training dataset and set $\lambda_w = 0.1$. For the backbone of the identity CNN, we tested the ResNet and lightweight MobileNet networks. For the critic network, we tested a 3-layer MLP with outputs of (60, 20, 1), while keeping the other settings fixed. The results in Table 2, show that using a shallower backbone for the identity CNN degrades the verification accuracy, while using a shallower critic network also reduces the verification accuracy, but to a lesser extent.

REFERENCES

- [1] Jiankang Deng, Jia Guo, Xue Niannan, and Stefanos Zafeiriou. ArcFace: additive angular margin loss for deep face recognition. In *Proceedings of the IEEE Conference on Computer Vision and Pattern Recognition (CVPR)*, 2019.

Algorithm 1: Training the WMI-AI age-invariant face embedding.

Algorithm input - face image x , age label τ_a , id label

τ_{id} .

Initialize the encoders and classifiers -

$f_a, f_{id}, D, g_a, g_{id}$

Set hyperparameters - $\lambda_w, \lambda_a, lr_w, lr$

foreach *epoch* **do**

Randomly select a batch x_i of size B

Compute $\hat{x}_{id} = f_{id}(x_i), \hat{x}_a = f_a(x_i)$

Set $\hat{x} = (\hat{x}_a, \hat{x}_{id}), \bar{x} = (\psi(\hat{x}_a)\psi(\hat{x}_{id}))$, ψ is the shuffle operator

foreach *step* w **do**

compute $L = L_w(\hat{x}, \bar{x}) - \lambda_g L_{grad}(\hat{x}, \bar{x})$

backpropagate D by maximizing L .

end **foreach**

Compute $L_w(\hat{x}, \bar{x})$

Compute $g_a(\hat{x}_a), g_{id}(\hat{x}_{id})$

Compute $L_a(g_a, \tau_a), L_{id}(g_{id}, \tau_{id})$

backpropagate g_{id}, f_{id} by minimizing

$L_{id} + \lambda_w L_w$

backpropagation g_a, f_a by minimizing $\lambda_a L_a$

end **foreach**

- [2] Zhizhong Huang, Junping Zhang, and Hongming Shan. When age-invariant face recognition meets face age synthesis: A multi-task learning framework. In *Proceedings of the IEEE Conference on Computer Vision and Pattern Recognition (CVPR)*, 2021.

- [53] Tianyue Zheng, Weihong Deng, and Jiani Hu. Cross-age LFW: A database for studying cross-age face recognition in unconstrained environments. *CoRR*, abs/1708.08197, 2017.

TABLE 2: Ablation of the backbone of the identity network and the critic networks. We report the verification accuracy [%] results.

Method	CALFW	AgeDB30	CACD-VS	ECAF(A,C)	ECAF(C,C)
WMI-AI+Resnet50	96.23	98.25	99.57	90.28	93.6
WMI-AI+Resnet34	96.13	98.1	99.55	89.98	93.3
WMI-AI+MobileNet	95.69	97.18	99.5	88.26	90.85
WMI-AI+smaller critic network	96.23	98.29	99.55	90.57	94.05
WMI-AI	96.26	98.37	99.57	90.73	94.40